nature biomedical engineering

ARTICLES

https://doi.org/10.1038/s41551-020-0557-2

Check for updates

A fidget spinner for the point-of-care diagnosis of urinary tract infection

Issac Michael[1,2,11], Dongyoung Kim[2,11], Oleksandra Gulenko[1], Sumit Kumar[2], Saravana Kumar[3], Jothi Clara[3], Dong Yeob Ki[1], Juhee Park[2], Hyun Yong Jeong[4,5,6], Taek Soo Kim[7], Sunghoon Kwon[4,5,8,9,10] and Yoon-Kyoung Cho[1,2] ✉

The point-of-care detection of pathogens in biological samples in resource-limited settings should be inexpensive, rapid, portable, simple and accurate. Here, we describe a custom-made fidget spinner that rapidly concentrates pathogens in 1-ml samples of undiluted urine by more than 100-fold for the on-device colorimetric detection of bacterial load and pathogen identification. In Tiruchirappalli, India, the device enabled the on-site detection of infection with the naked eye within 50 min in urine samples from 39 patients suspected of having a urinary tract infection. We also show that, in 30 clinical samples of urinary tract infection, the device can be used to perform an antimicrobial susceptibility test for the antimicrobial drugs ciprofloxacin and cefazolin within 120 min. The fidget spinner could be used in low-resource settings as an inexpensive handheld point-of-care device for the rapid concentration and detection of pathogens in urine samples.

In resource-limited settings, conventional medical devices used in modern laboratories face obstacles such as interrupted power supplies, a shortage of skilled professionals, adverse environmental conditions and the absence of rapid data connectivity. In such circumstances, clinical decisions are based on symptoms rather than diagnostic tests, leading to complex clinical complications[1–4]. Several types of point-of-care-testing (POCT) devices for the diagnosis of infectious diseases have been developed but not all can be utilized in resource-limited settings[5–11]; the costs, a lack of trained technicians and requirements for additional instrumentation are a few practical obstacles[11–13]. Lateral flow strip sensors are advantageous in such situations but have restrictions in terms of their sample volume, thereby creating the need for new tools[14,15].

Urinary tract infection (UTI) is a common disease across the world, leading to healthcare costs worth millions of dollars and affecting over 50% of women worldwide before they reach the age of 32 yr[16–18]. During pregnancy, UTIs are common and can be dangerous without adequate screening and treatment[19]. For patients with clinical UTI symptoms, the standard diagnosis is based on pathogen detection using urine cultures (Fig. 1a; Conventional)[15,20]. The required infrastructure for this is unfortunately absent in many rural areas; hence, clinicians resort to symptom-based diagnosis, which results in the prescription of broad-spectrum antimicrobial treatment for an unknown infection. Urinary-tract-infection dipstick tests are available but are known to be less reliable than urine culture tests. This practice harms the healthy microbiome of the patient and leads to antimicrobial resistance[21].

A fidget spinner is a handheld toy that can spin freely when pushed[22]. It consists of a roller bearing in the middle and two or three weighted lobes. The fidget spinner is rotated by holding the centre pad and pushing a lobe with the other hand (Fig. 1b, left and Supplementary Video 1). It can spin for more than 1 min with minimal effort. Based on this idea of a device spinning like a centrifuge, we designed a centrifugal microfluidic device by adapting the working principles of a fidget spinner. Centrifugal force is the major driving force in such a device, which depends on the size and rotational speed of the device. Non-conventional electricity-free centrifugal-force-based devices have been reported[23–25]. To the best of our knowledge, previously developed non-conventional electricity-free centrifugal-force-based devices can be used for simple unit operations such as blood separation on the device[23,25] or integrated multiplex assays[24]; however, they required additional off-chip sample preparation or assays for target detection. Here, the proposed device operated by hand power enables a 'sample-in-and-answer-out' type of function with sample enrichment capability for high sensitivity detection with the naked eye without the need for additional instrumentation, which is important in point-of-care diagnostics, especially in settings with limited resources. The fidget spinner, which is inexpensive, palm-sized, simple in design, robust and easy to operate, can be a good platform for a fully integrated sample-in-and-answer-out diagnostic device with built-in sample preparation capability[13,26,27].

Considering the above factors, we engineered a diagnostic tool that works like a fidget spinner—that is, a diagnostic fidget spinner (Dx-FS). The Dx-FS is an instrument-free lab-on-a-disc platform that can provide a low-cost electricity-free UTI diagnosis (Fig. 1a; Dx-FS). When the Dx-FS is spun, the bacteria suspended in the sample are enriched on a nitrocellulose membrane and can be

[1]Department of Biomedical Engineering, School of Life Sciences, Ulsan National Institute of Science and Technology (UNIST), Ulsan, Republic of Korea. [2]Center for Soft and Living Matter, Institute for Basic Science (IBS), Ulsan, Republic of Korea. [3]Kauvery Hospital Pvt. Ltd., Tiruchirappalli, India. [4]Department of Transdisciplinary Studies, Seoul National University, Seoul, Republic of Korea. [5]Institutes of Entrepreneurial BioConvergence, Seoul National University, Seoul, Republic of Korea. [6]BK21+ Creative Research Engineer Development for IT, Seoul National University, Seoul, South Korea. [7]Department of Laboratory Medicine, Seoul National University Hospital, Seoul, Republic of Korea. [8]Department of Electrical and Computer Engineering, Seoul National University, Seoul, Republic of Korea. [9]Biomedical Research Institute, Seoul National University Hospital, Seoul, Republic of Korea. [10]Quantamatrix Inc., Medical Innovation Center, Seoul National University Hospital, Seoul, Republic of Korea. [11]These authors contributed equally: Issac Michael, Dongyoung Kim. ✉e-mail: ykcho@unist.ac.kr

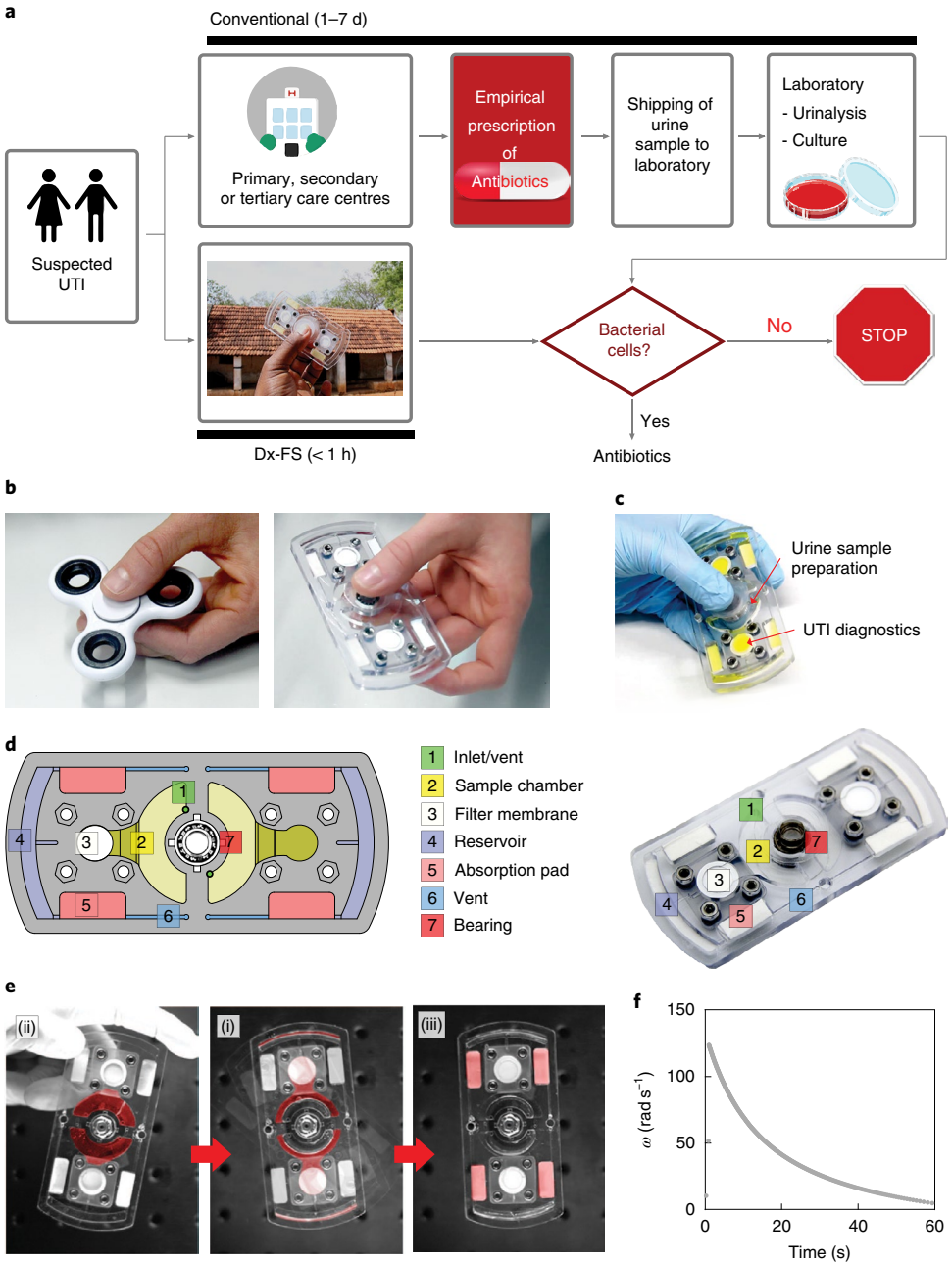

Fig. 1 | The Dx-FS as a POCT device for low-resource settings. a, In developing countries such as India, healthcare is classified into three levels: primary, secondary and tertiary care. Although secondary and tertiary care centres are equipped with laboratories for UTI screening, the same does not exist in primary care centres[34,35]. Patients seeking intervention with symptoms of UTI predominantly visit primary care centres, and medication is prescribed based on the symptoms rather than a clinical diagnosis. The flowchart shows the diagnosis of UTIs in rural areas by the conventional method that takes about a week, which includes healthcare visits, empirical antibiotic prescription, urine shipment to the laboratory, and urinalysis and culturing at the laboratory. A Dx-FS may process a urine sample in less than 1 h and obtain equivalent results. **b**, Fidget spinner (left) and Dx-FS (right). **c**, Sample enrichment (urine sample preparation) and UTI diagnostics performed by a Dx-FS. **d**, Design of the Dx-FS with labelled parts. **e**, Images from a high-speed video showing the operation of a Dx-FS: the device was (i) hand-spun, (ii) spun for 1 min and (iii) stopped. The areas coloured in red denote the liquid flow during the process. **f**, Angular rotational frequency of the Dx-FS versus time.

detected with the naked eye through colorimetric microbial detection within 50 min. As the Dx-FS is hand-powered, only a limited centrifugal force is available, which is highly variable depending on the operator. We overcame this problem by using a pressure equalization technique. For validation, a field test was performed in India. Urine samples from 39 patients with clinical symptoms of a UTI were tested using a Dx-FS and the results were compared with those from the conventional culture method. Our results showed that a Dx-FS can inform the presence of viable cells in urine within 50 min in contrast to turnaround times of several days. In a clinical context this would help to identify patients requiring antimicrobials among those who are symptomatically suspected. To expand the scope of the clinical utility of the Dx-FS, we performed a simplified antimicrobial susceptibility test (AST; Fidget-AST) that allowed the testing

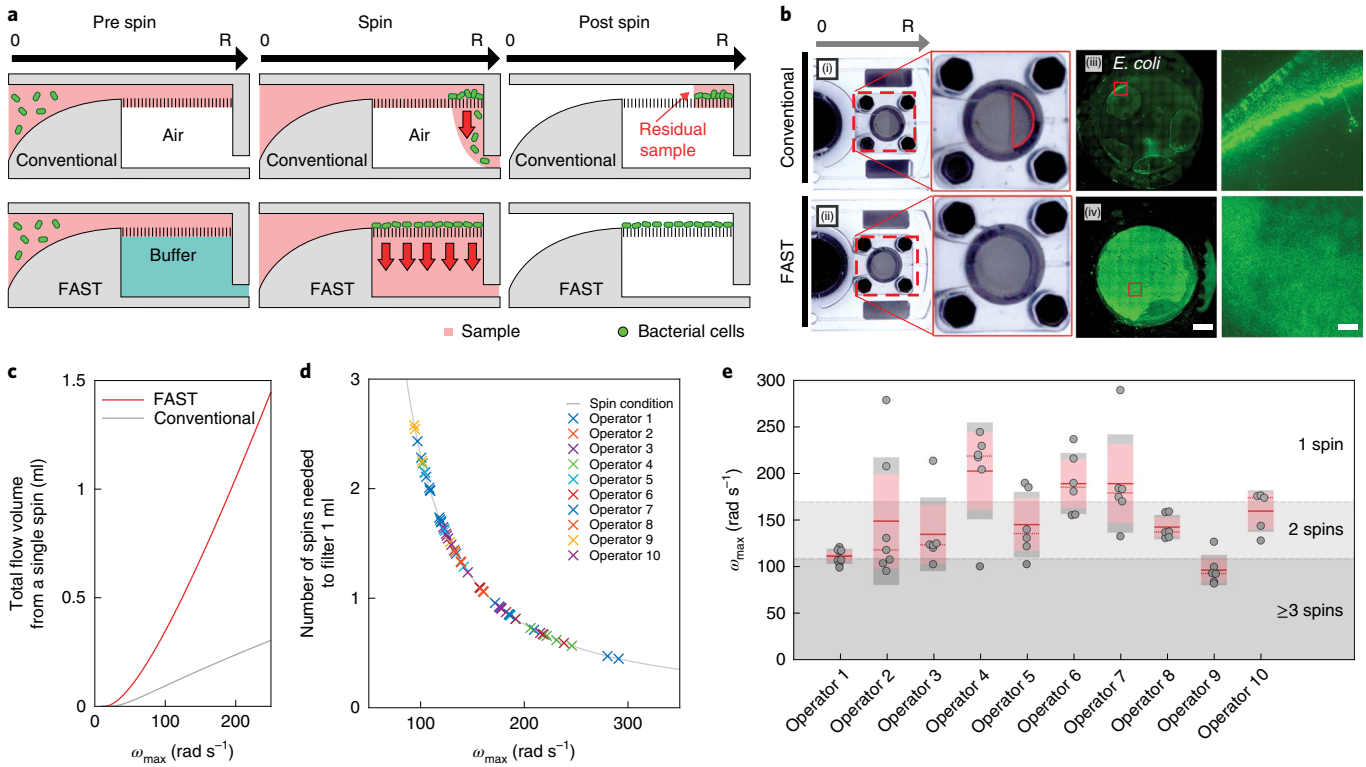

Fig. 2 | Characterization of the fluid flow and operation of a Dx-FS. a, Schematic of the cross-sectional view of a Dx-FS device depicting bacterial enrichment of a sample through the filter membrane in the conventional (top) and FAST (bottom) setups. In the FAST-based particle separation (bottom), the fluid flow caused by the centrifugal force is perpendicular to the filtration flow through the membrane, similar to the tangential flow-filtration case. In addition, the drainage chamber underneath the membrane remains fully filled with the liquid during the entire filtration process (also refer to Kim et al.[28] for details). This is achieved by placing a buffer solution in the bottom chamber of the membrane before the spinning process, which ensures uniform filtration across the entire area of the membrane and significantly reduces the hydrodynamic resistance. R, radial direction. **b**, Images showing effective filtration during rotation (left) and fluorescence images of bacterial cells (right) enriched on the membrane for conventional ((i) and (iii)) and FAST ((ii) and (iv)) filtration. Scale bars, 2 mm (left) and 0.1 mm (right; magnified view). **c**, Flow volume of the Dx-FS estimated at ω_{max}. **d**, Number of spins performed by ten independent individuals who spun a Dx-FS. The angular velocities were measured, and the number of spins to elute 1 ml of liquid was estimated. **e**, Measurements from **d** plotted for each Dx-FS operator (operators 1 and 2, $n = 7$, all other operators, $n = 6$). The red lines, dashed red lines, and grey and red boxes over the measurements (grey dots) denote the mean, median, s.e.m. and s.d., respectively. The grey areas indicate the number of spins in **d**.

of susceptibility to antimicrobials within approximately 120 min. The results obtained from 30 clinical isolates from 30 patients with a UTI confirmed that a Fidget-AST could be a viable alternative to conventional ASTs in resource-limited settings.

Results

Enrichment of bacteria with a few spins. By combining the working principles of centrifugal microfluidics and a fidget spinner, we developed an easy-to-use hand-powered spinning device to perform diagnostic tests devoid of electricity and complex instruments (Fig. 1). The Dx-FS is a POCT device that assimilates sample preparation and detection (Fig. 1b, right). The Dx-FS retains the simple operation principle of a fidget spinner; the centre pad is held between the thumb and the index finger while the edge of the device is pushed with the other hand (Supplementary Video 1). This allows for user-friendly operation over a wide range of audiences. In this study, we applied our device to perform UTI diagnoses (Fig. 1a,c). By adding 1 ml of a urine sample to the Dx-FS and spinning the device by hand, the pathogens from the sample were filtered and detected using an assay that can provide information on the live bacterial load within 50 min. Detailed descriptions of the design (Fig. 1d), fabrication (Supplementary Fig. 1) and sequence of fluid flow during the operation of Dx-FS (Fig. 1e) are presented in Methods.

The Dx-FS harnesses the kinetic energy imparted by hand when pushed and converts it into a centrifugal force (Fig. 1e and Supplementary Video 1). Unlike motor-driven centrifugal devices, the Dx-FS relies on the strength of each individual operator, which typically generates an angular rotational frequency (ω) smaller than 300 rad s^{-1}. Figure 1f shows the measurements of the ω for a Dx-FS over time (see Methods and Supplementary Fig. 2). As the edge of the device is pushed by a finger, it quickly reaches a maximum angular rotational frequency (ω_{max}) and then slows down over the course of a minute.

Despite the relatively low spinning speed with large variations, the filtration efficiency of the Dx-FS is high owing to fluid-assisted separation technology (FAST[28]; Fig. 2). However, in a conventional non-FAST case, where the space below the membrane is partially filled with air, a non-uniform pressure difference across the membrane is produced, which makes filtration possible only through the most vulnerable point (the highest pressure difference). In such cases, the speed of the hand-powered spin is not sufficiently high, resulting in a substantial volume of the sample remaining on the membrane (Fig. 2a, Post-spin and Fig. 2b(i), marked in red). However, no residual sample was observed for the FAST (Fig. 2b(ii)). We observed a non-uniform distribution of bacteria in the conventional filtration, which implies that the non-uniform fluid-flow deposits concentrate the bacterial cells on the high-pressure area of the

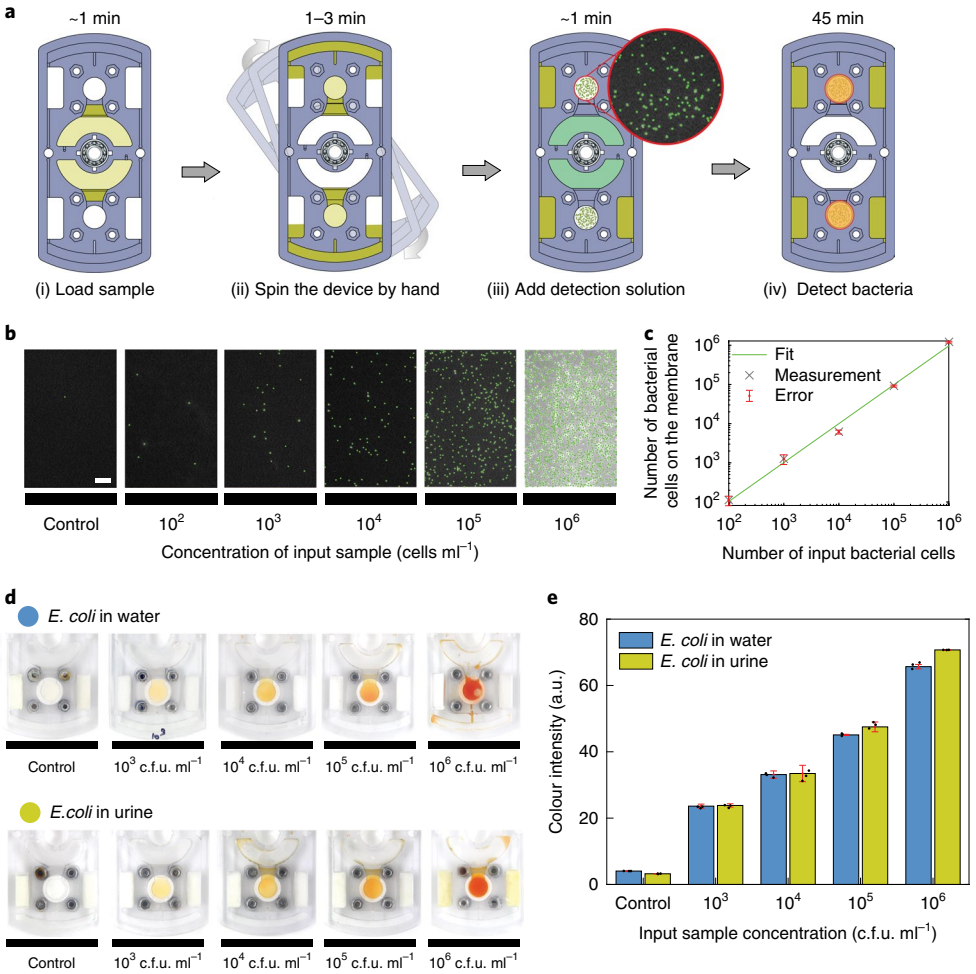

Fig. 3 | The Dx-FS as a versatile bacterial infection diagnostic platform. a, Operation of a Dx-FS device preloaded with FAST solution (Supplementary Fig. 7): (i) a sample is loaded into the sample chamber, (ii) spinning allows the sample to flow through the membrane, (iii) the detection solution is added, followed by incubation and (iv) bacterial cell contamination is visualized as an orange colour. **b**, Fluorescently labelled bacterial cells enriched using a Dx-FS. The membranes were imaged by fluorescence microscopy ($n=3$ per condition). Scale bar, 20 μm. **c**, Number of bacterial cells detected on the membranes shown in **b**. The centre value of the mean from three repeats is shown as an x, and the error is denoted as standard deviation. **d**, Colorimetric bacterial cell viability assay performed using a Dx-FS. Water (top) and a urine sample (bottom) were spiked with bacterial cells. **e**, Orange colour intensities from **d**. The colour intensities were measured and the averages (bars) and s.d. (error bars) were plotted ($n=3$). Two standard methods for bacterial counting were used—that is, haemocytometer and bacterial-cell-colony counts after culturing (c.f.u.)—and the colorimetric calibration of the bacterial cell count and c.f.u. are given in Supplementary Fig. 10. According to the UTI guidelines provided by the Centers for Disease Control and Prevention, the clinical threshold level for positive UTI diagnostics is a bacterial load level greater than 1×10^5 c.f.u. ml^{-1} in addition to clinical symptoms[5,28]. Furthermore, the American Society of Microbiology and the European urinalysis guidelines[29] state that a UTI occurs when the bacterial load in urine reaches 1×10^3 c.f.u. ml^{-1}, when most UTI-related symptoms appear[31,32]. a.u., arbitrary units.

filter (Fig. 2b(iii)). Using FAST, we could achieve uniform spreading of bacterial cells on the porous filter, as it uses the entire membrane (Fig. 2b(iv) and Supplementary Fig. 3), where the intensity is 11.6× higher than the non-FAST method. Owing to uniform filtration, the flow rate during filtration was also enhanced, as shown in Fig. 2c and Supplementary Fig. 4. Furthermore, we tested liquid samples with various densities and levels of bacterial contamination and confirmed that such conditions do not affect the flow rate during the operation of a Dx-FS (Supplementary Fig. 5).

Another challenge associated with hand-powered centrifugation is that each operator may use a different amount of power to spin the device. To measure this difference, individuals across different age groups (19–45 yr) were asked to perform the spinning operation. Figure 2d,e summarizes the ω_{max} measurements of the Dx-FS for ten Dx-FS operators in multiple trials. We measured ω_{max} in the range of 90–300 rad s^{-1} from 62 measurements, with an average ± s.d. of 151 ± 48 rad s^{-1} (Fig. 2d). There were large variations in the spin speed among the Dx-FS operators and during trials (Fig. 2e). Here, we found that more than 12 manual spins were required to filter 1 ml of the sample in conventional centrifugation. However, only one or two manual spins were sufficient to decant the same volume of the sample using a FAST-enabled Dx-FS, which requires approximately 1–3 min. The completion of the filtration process was confirmed by visual inspection of the empty filter chamber. Overall, we confirmed that a Dx-FS equipped with FAST-based filtration helps to achieve robust, fast and efficient bacterial enrichment with minimal human effort.

Dx-FS as a POCT platform. The Dx-FS was developed and optimized as a POCT device for UTI detection, and it can be utilized in remote areas, where centralized laboratory facilities, uninterrupted power supplies and expert personnel are absent. The Dx-FS

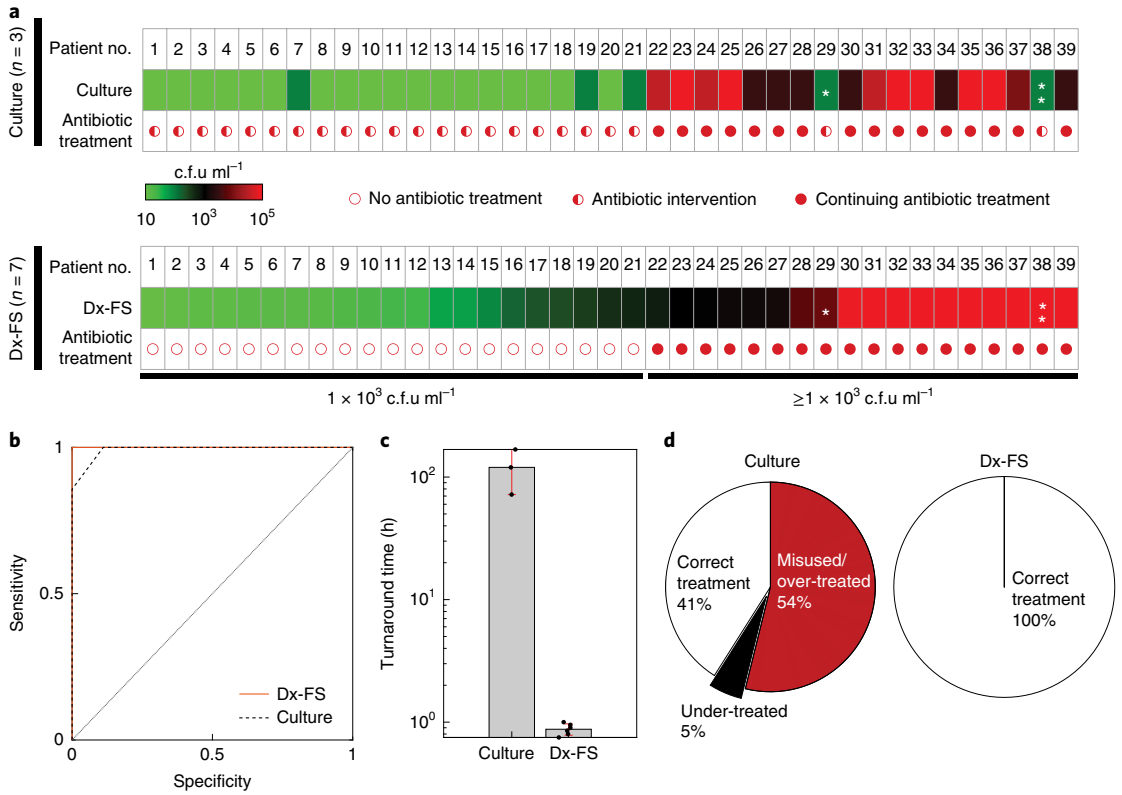

Fig. 4 | Proof-of-concept testing using the Dx-FS. a, Urine samples from patients with a suspected UTI were tested by culturing and using a Dx-FS. The bacterial cell counts measured through both culturing and a Dx-FS are shown as a heat map. The diagnoses of medical doctors are indicated by the red circles. *Urinalysis of Patient 29 showed 15 pus cells per HPF in the urine; **urinalysis of Patient 38 showed 15 RBCs per HPF and 5 pus cells per HPF in the urine. **b**, ROC curves of the UTI diagnoses obtained from culturing and Dx-FS. The Dx-FS results are highly comparable to the conventional culture-based UTI diagnoses in terms of sensitivity and specificity. **c**, Average ± s.d. turnaround times of the culturing ($n = 3$) and Dx-FS ($n = 7$) methods. Culturing takes >120× longer than a Dx-FS. **d**, Results of our simulation of antibiotic treatments. The results indicate that 54% of patients with a suspected UTI misused the antibiotics or were overtreated with antibiotics, 5% of patients with a UTI were undertreated (* and ** from **a**), and 41% of patients with a UTI were treated correctly (left). In contrast, the Dx-FS could help provide all patients with the correct treatment (right).

is a cost-effective, disposable and user-friendly POCT device with an integrated sample-preparation function to provide a detection sensitivity equivalent to that of a clinical laboratory. The estimated material cost for a Dx-FS kit capable of testing two samples is US$0.48 (Supplementary Table 1 and Supplementary Fig. 6), which can be reduced when scaling up production.

For the practical utility of the Dx-FS as a POCT platform, we simplified the overall operation to three manual steps: raw sample injection, bacterial enrichment and final detection (Fig. 3a and Supplementary Video 2). First, 1 ml of a raw urine sample is introduced into the device, preloaded with FAST solution (Supplementary Fig. 7), using a plastic pipette through the inlet hole (Fig. 3a(i)). The bacterial cells in the urine sample are enriched by spinning the device (Fig. 3a(ii)). Spinning is repeated until the sample is completely filtered. Finally, the FAST solution is removed to retain the detection solution on top of the membrane, followed by addition of the detection solution (see Methods), which is then spun for a short interval until the solution is localized to the membrane chamber (Fig. 3a(iii)). The colour change is measured after 45 min and translated into bacterial load (Fig. 3a(iv)).

We first evaluated the dynamic range of the device using synthetic urine samples spiked with bacteria at a concentration range of 0–1×10^6 cells ml^{-1} *Escherichia coli*. The membranes were observed under a fluorescence microscope (Fig. 3b). Quantification from the fluorescence microscopy images confirmed that a Dx-FS could filter 99.35% of bacterial cells in a 1 ml sample with a concentration range of 1×10^2–1×10^6 cells ml^{-1} *E. coli* (Fig. 3c). Here, the bacterial cells were enriched on the filter membrane, which eventually reduced the sample volume from 1 ml to <8 µl, resulting in a concentration more than 126.5× higher than that of the input sample (Supplementary Fig. 8).

To facilitate easy interpretation for users, we integrated a proven rapid colorimetric WST-8 assay[29]—in which the electron mediator in the kit receives electrons from viable bacterial cells and transfers them to the WST-8, causing changes to the orange colour of the formazan dye that can be visually identified with the naked eye—into the Dx-FS (Supplementary Figs. 9 and 10). Samples with bacterial concentrations of 1×10^3–1×10^6 colony-forming units (c.f.u.) ml^{-1} were tested to confirm the effective range of detection. A semi-quantitative estimate of the bacterial load can be easily obtained by visual comparison to a colour chart following detection with the naked eye (Fig. 3d and Supplementary Fig. 11). Without the enrichment step, the signal was too low to detect a bacterial concentration of 1×10^5 c.f.u. ml^{-1} (Supplementary Fig. 12). For further quantitative characterization of the device, images of the Dx-FS with bacterial loads in the range of 1×10^3–1×10^6 c.f.u. ml^{-1} were analysed and plotted (Fig. 3e and Supplementary Fig. 13). Furthermore, we confirmed that the microbial viability assay kit used is highly favourable for bacterial cells with the use of a specific electron mediator[30]. There was no notable signal from mammalian cells (<10^5 cells ml^{-1}; Supplementary Fig. 14 and Supplementary Note 1). The assay operates at temperatures above 30 °C; however, a hand

warmer can be helpful in colder environments (Supplementary Fig. 15 and Supplementary Note 2). No significant difference in colour was observed after 24 h after the detection was performed (Supplementary Fig. 16). Based on all these observations, we conclude that the Dx-FS is a versatile platform that meets the WHO (World Health Organization)-ASSURED standards (Supplementary Table 2); therefore, the Dx-FS can be an effective diagnostic tool for POCT in resource-limited settings.

Field trial in India. To evaluate how the Dx-FS fits the clinical needs in a resource-limited setting, we performed a field trial of the Dx-FS in Tiruchirappalli, India, where the majority of patients come from rural areas (Fig. 1a). Patients seeking intervention with symptoms of a UTI predominantly visit primary care centres and are prescribed medication based on the symptoms rather than a clinical diagnosis. Select cases are subjected to traditional clinical diagnosis—such as a microscopic examination, dipstick assay and cultures—in a laboratory located in an urban setting. Generally, empirical antimicrobial therapy is administered by the primary care centre as per the guidelines for a community-acquired UTI[31]. Studies on a large population of UTI-affected patients have concluded that symptom-based UTI diagnoses place a large number of patients at risk by prescribing unnecessary antimicrobials[30–34]. Although the practice is well-established and convenient for the treatment of many patients who predominantly visit primary care centres, it contributes substantially to antimicrobial resistance.

In our approach, we attempted to minimize the time and associated cost of conventional UTI diagnosis, and prevent the misuse of antimicrobials by providing clinical information regarding bacterial load within 50 min (Fig. 1a, Dx-FS). We tested urine samples from 39 patients who enrolled during 1–17 August 2018 (Supplementary Table 3). The samples were collected and processed according to the regulations of the Clinical Trial Registry–India, and all experiments were performed in a microbiology laboratory within the hospital (Supplementary Fig. 17). The samples were processed using two different methods: conventional (urinalysis and culturing at a hospital laboratory) and Dx-FS (Fig. 1a and see Methods). Patients that had bacterial concentrations $\geq 10^3$ c.f.u. ml^{-1} in their urine were considered UTI-positive according to the hospital standards (European urinalysis guidelines)[35]. The measurements from all 39 patients are shown in Fig. 4a. Twenty-three patients with a suspected UTI (59%) tested negative according to the bacterial cell cultures (Patients 1–21, 29 and 38; Fig. 4a, culture), whereas 21 patients with a suspected UTI (54%) had bacterial concentrations $\leq 10^3$ c.f.u. ml^{-1} in their urine according to the Dx-FS test (Patients 1–21; Fig. 4a, Dx-FS). For Patient 29, >15 pus cells (leukocytes) per high-power field (HPF) were detected; for Patient 38, >15 red blood cells (RBCs) per HPF and over five pus cells per HPF were detected at the subsequent urinalysis (Fig. 4a; * and **, respectively). Such pus cell or RBC counts in urine indicate infection and urinary tract damage; therefore, antimicrobial treatments are needed[21]. Except for Patients 29 and 38, whose samples indicated many (≥15) pus cells or RBCs, other urine samples could be cultured despite the fact that they contained moderate levels of pus cells ($5 \leq$ pus cell < 15) or many RBCs (≥15). The results confirm that UTI diagnoses from the cultures and Dx-FS were comparable (Fig. 4b). The Dx-FS provided a robust and versatile UTI diagnosis independent of the gender and age of the patient as well as the strain of the bacterial cells (Supplementary Fig. 18). According to the culturing results, 54% of the patients with a suspected UTI did not have a UTI. Moreover, 5% of the patients with a suspected UTI who tested negative according to the culture still needed antimicrobials (Fig. 4d). In the Dx-FS-based POCT scenario, the presence of bacterial cells in urine can be identified within 50 min (Fig. 4c, Dx-FS); therefore, instead of treating all of the patients with a suspected UTI with clinical symptoms, it is possible to treat only the patients who had pathogen detected with antimicrobials. The empirical antimicrobial treatment of non-UTI patients could have undesirable side effects, paving the way to drug resistance.

Fidget-based AST. A rapid point-of-care-based AST that can help to identify the right drug among the recommended few can reduce further complications in antimicrobial resistance at the primary care level[36,37]. A conventional AST performed in a laboratory setting is based on bacterial culturing, which takes at least two working days (Fig. 5a); this is not feasible in point-of-care applications[38]. As the major UTI cases diagnosed in primary care centres are caused by *E. coli* (>80 %), we focused on this species. On confirming that the pathogen is *E. coli* by enriching the pathogen using a Dx-FS, followed by pathogen-identification techniques such as molecular assays using isothermal amplification such as recombinase polymerase amplification followed by a lateral flow assay (Supplementary Fig. 19 and Supplementary Note 3) or an immunoassay using gold nanoparticles (Supplementary Fig. 20 and Supplementary Note 4), a rapid Fidget-AST can be performed as demonstrated in Fig. 5. Note that all assays allow detection with the naked eye.

To demonstrate the feasibility of performing a Fidget-AST under primary care settings, we compared the colour intensity of the bacterial population that was exposed to drugs with the control, thereby categorically identifying susceptible and resistant bacteria within 120 min (Fig. 5a,b). If the viable-bacteria signal measured by the Dx-FS for the antibiotic-treated sample is substantially reduced, it suggests that these bacteria are susceptible to the antibiotic drug. As a proof of concept, bacterial cells from 30 UTI patients (Supplementary Table 4) were tested with two antimicrobial drugs, ciprofloxacin (CIP) and cefazolin (CZ) at minimum inhibitory concentrations (MIC) recommended by the Clinical and Laboratory Standards Institute (CLSI) for *E. coli*—1 μg ml^{-1} and 4 μg ml^{-1} for CIP^{Low} and CIP^{High}, respectively, and 16 μg ml^{-1} and 32 μg ml^{-1} for CZ^{Low} and CZ^{High}, respectively—to identify drug-susceptible or -resistant bacteria. Figure 5c shows the results of the Fidget-ASTs performed under four conditions: susceptible to both, CIP susceptible and CZ resistant, CIP resistant and CZ susceptible, and resistant to both, with both positive and negative controls. The positive controls

Fig. 5 | Antimicrobial susceptibility test for clinical isolates using a Dx-FS. a, A conventional AST takes a minimum of 2 d for the cell culture and AST; however, a Fidget-AST to check phenotypic resistance takes less than 120 min. **b**, Schematic of the Fidget-AST procedure developed for clinical urine samples. (i) The urine sample is tested with a Dx-FS for bacterial load (45 min) and bacterial cell identification by recombinase polymerase amplification followed by a lateral flow assay (Fidget-ID, 30 min) in parallel. (ii) If the sample contains a specific strain (for example, *E. coli*), an antibiotic drug is mixed with the sample for 20 min, followed by a Dx-FS microbial detection assay for 45 min to check drug susceptibility. **c**, Summary of the Fidget-AST results obtained for the clinical urine samples studied in this work. Two antibiotic drugs, CIP and CZ, were tested in two dosages according to CLSI guidelines. Four cases of both CIP- and CZ-susceptible (S/S, $n=15$), CIP susceptible and CZ resistant (S/R, $n=5$), CIP resistant and CZ susceptible (R/S, $n=5$), and both CIP- and CZ-resistant (R/R, $n=5$) clinical urine samples were tested ($n=3$). Pos., positive control; Neg., negative control. **d**–**f**, Colour-intensity measurements of the four cases in 30 clinical samples (**d**), and for the susceptible and resistant cases (**e**). **f**, ROC analysis. The dotted lines (**d**,**e**) denote the cutoff estimated from the ROC analysis (**f**). Significance was tested using a two-sided Student's *t*-test; $***P = 6.0064 \times 10^{-21}$. For each box plot, the central red mark indicates the median, and the bottom and top edges of the box indicate the 25th and 75th percentiles, respectively. The whiskers extend to the most extreme data points that were not considered outliers.

and resistant cases showed a strong orange signal, suggesting no substantial changes in the concentration of viable bacterial cells, whereas the negative controls and susceptible cases showed weak orange signals, indicating a reduction in the number of live bacteria. The second-generation antimicrobial CIP, which has become a common drug for UTI treatment, acts on *E. coli* by inhibiting DNA gyrase; however, the first-generation antimicrobial CZ acts on the cell wall and causes it to lyse. The colorimetric WST-8 assay in the Dx-FS measures the dehydrogenase activity of bacterial cells, which is closely related to the cell metabolic activity. We therefore concluded that antimicrobial exposure of the bacterial cells inhibits the overall cell metabolic activities and changes the colour intensity.

Colour differences were clearly distinguishable with the naked eye, and the colour intensities obtained from 30 patient samples are

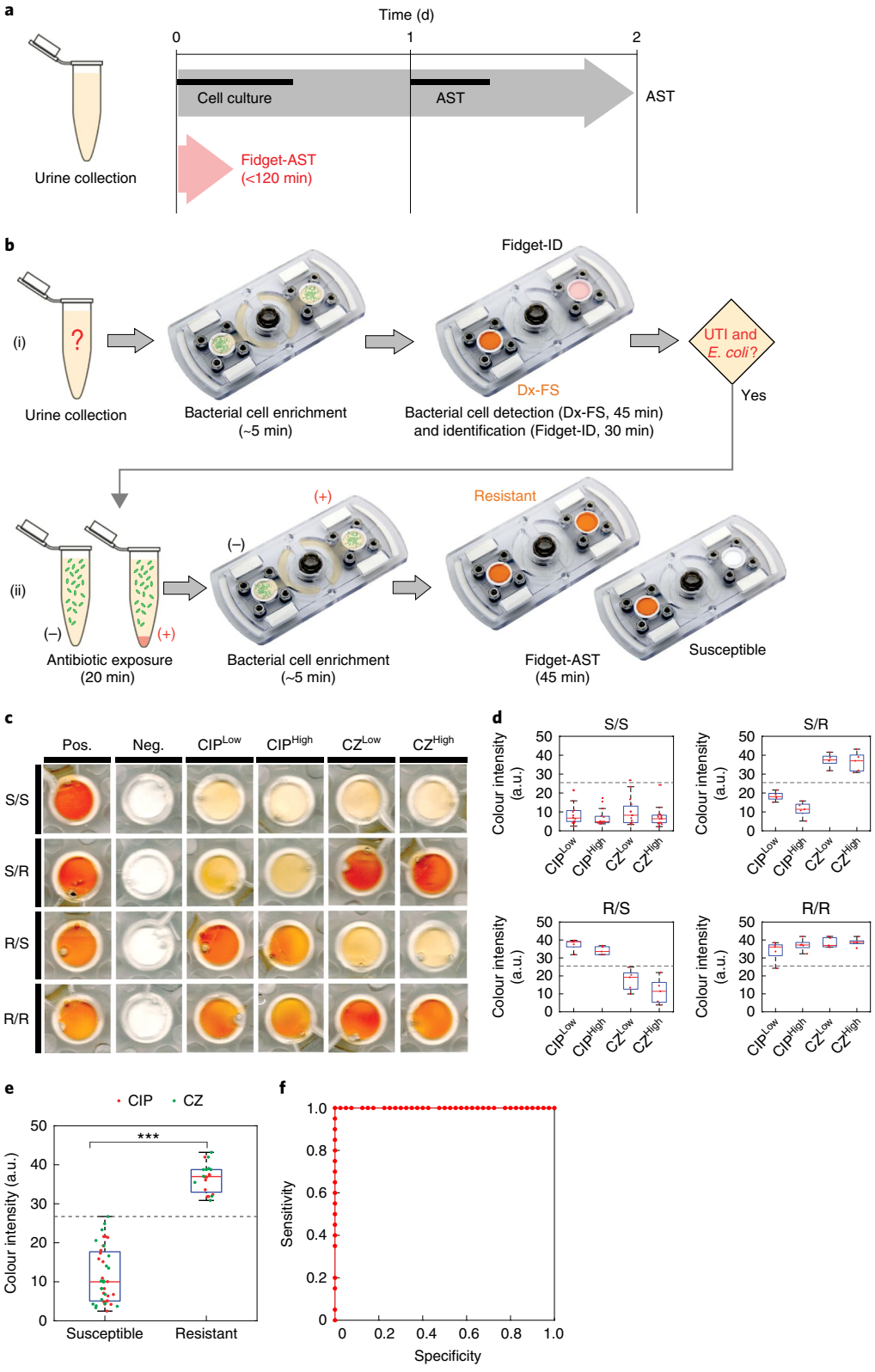

shown in Fig. 5d. We further analysed the measurements considering the susceptible and resistant samples (Fig. 5e). A clear difference between the two groups was observed, with a cutoff of 27 a.u., from the receiver operating characteristic (ROC) analysis (Fig. 5f). Although conventional AST remains the gold-standard method, the Fidget-AST can offer a quick and simple alternative method to determine the phenotypic antimicrobial susceptibility for the common UTI cases at point-of-care settings. We focused on identifying the right antimicrobial among the empirical ones that is of best interest to the infected patients at point-of-care settings.

Discussion

We have demonstrated that a Dx-FS can be easily operated and a bacterial load of 1×10^3 to 1×10^6 c.f.u. ml^{-1} can be determined, which is useful to avoid unnecessary antimicrobial usage. A field test of Dx-FS was conducted in Tiruchirappalli, India, where a large proportion of patients diagnosed with a UTI worldwide are located[1–3]. The test with 39 patient samples confirms that symptom-based diagnosis combined with a Dx-FS can identify patients who need antimicrobials, thereby reducing antimicrobial misuse. The study was planned and executed with input from doctors in local hospitals in India, who are aware of the clinical needs in resource-limited settings. In addition, a rapid AST in a Dx-FS was performed to identify the susceptibility of the bacteria to two antimicrobials within 120 min. Compared with conventional AST methods, a Fidget-AST can be performed instrument free by someone with minimal training.

The Dx-FS is a palm-sized device powered by hand, which has an intrinsic limitation of a slow and varying rotational speed. We overcame this problem by engineering the flow dynamics within the device using FAST[28]. The FAST approach equalizes the pressure difference between the top and bottom of the membrane, thereby substantially reducing the overall hydrodynamic resistance. Consequently, rapid liquid transfer through the membrane was achieved within the range of centrifugal forces provided by hand spinning. In the case of incomplete filtration of the 1 ml sample in a single spin, it is recommended to repeat the spinning until complete filtration occurs; this can be confirmed by visual inspection of the filter chamber. The entire filter membrane is evenly used during filtration, which ensures robust sample enrichment under various spinning conditions. While the FAST mechanism allows rapid filtration, we utilized the advantage of the non-FAST method to retain detection solution at very low volumes above the filtration membrane by withdrawing the fluid from the bottom chamber underneath the membrane just before introducing the detection solution.

We demonstrated the effectiveness of the Fidget-AST in categorizing viable bacteria from patient samples with and without antimicrobial treatment through detection with the naked eye using the WST-8 assay. Although the WST-8 assay is suitable for the quantification of live bacteria, it is not applicable to specific pathogen identification. Taking advantage of the pathogen-enrichment capability of a Dx-FS, other methods of detection with the naked eye that perform sensing based on isothermal amplification (Supplementary Fig. 19) or immunoaffinity (Supplementary Fig. 20) can be used to identify the specific type of pathogen. We would like mention that the current proof-of-concept study involved only *E. coli*, which is estimated to cause 80% of UTIs. Further tests should be performed in the future for other bacterial species such as *Klebsiella pneumoniae* or *Proteus mirabilis*.

The gold standard for UTI diagnosis is urine culture and urinalysis, which cost up to US$250 per test along with 2–3 d of experiments, depending on the depth of the panel (for example, LabCorp). There are UTI POCT devices that have been approved by the US Food and Drug Administration—for example, a device from BacterioScan that identifies negative infection samples within a turnaround time of 3 h. These devices may be useful in a hospital setting to improve the efficiency of laboratory work but they are not feasible for remote settings. Proposals to use syringe filtration for UTI diagnosis might lead to the development of simple POCT devices[39,40]. However, such devices require additional instrumentation and can be labour intensive. This too is impractical for POCT devices in resource-limited settings. Our Dx-FS can be used to perform a UTI diagnosis in 50 min with no additional device or electricity requirements, and the material costs for a Dx-FS kit is estimated to be US$0.48 (Supplementary Table 1). The WHO sets ASSURED criteria for an ideal POCT device, which should be affordable, sensitive, specific, user-friendly, rapid, robust, equipment-free and delivered to those who need it[41]. In addition, POCT devices need to be used in non-hospital settings with data connectivity to support follow-up care and public health efforts. Overall, the results demonstrate that the Dx-FS is a disruptive technology that meets the need for UTI management using POCT devices, especially in resource-limited settings.

Methods

Design and working principles of the Dx-FS. The Dx-FS incorporates three functional parts: a sample loading chamber, filtration unit and reservoir (Fig. 1d). First, the sample is loaded into the sample loading chamber (2, Fig. 1d) through the inlet (1, Fig. 1d). Here, the device is designed to hold a maximum of 1.2 ml in a single unit. By holding the centre part of the device comprising a roller bearing (7, Fig. 1d), the device is spun, the resulting centrifugal force drives the sample and assists with filtration through a nitrocellulose membrane (3, Fig. 1d) and the residual liquid is collected in the reservoir (4, Fig. 1d). The membrane in the device was strategically positioned to face the top, thereby providing the user with direct visualization of the colorimetric result and allowing for microscopic examination of the pathogens captured on the membrane. The residual fluid in the reservoir is removed by an absorption pad (5, Fig. 1d). Figure 1e shows the sequence of fluid flow during the operation of the Dx-FS. When the device is set to spin, the sample (coloured in red) in the loading chamber experiences a centrifugal force (Fig. 1e(i)) that pushes the fluid through the membrane (Fig. 1e(ii)). The residual liquid is removed by the absorption pad when the device spins slowly or is halted, which prevents sample leakage through the vent holes. This is achieved by the capillary wicking introduced along with the centripetal forces (Fig. 1e(iii)).

Fabrication of the Dx-FS. The dimensions of Dx-FS are 106 mm × 50 mm × 5.5 mm (length × width × thickness) (Supplementary Fig. 1). The average length of an adult hand, for both men and women, was considered, and the device was fabricated to fit well within the hand and be conveniently operated. Tests were carried out with ten operators (five men and five women) aged 19–45 yr and the design was finalized. Metal bearings with an outer diameter of 18 mm were chosen, as they were small and ideal for providing a large area for the device. A Dx-FS comprises three layers—that is, a 5-mm-thick polycarbonate sheet (I-Components, Co., Ltd.) as the main body, a 0.1-mm-thick double-sided adhesive layer (DFM 200 clear 150 POLY H-9 V-95; FLEXcon) in the middle and a 0.125-mm-thick transparent polycarbonate layer on top. A digital design was created using three-dimensional computer-aided design (CAD) software (SolidWorks, 2015), and the main body was carved on both sides using a computer-numerical-control milling machine (Promill Smart 3530, Protek). The top-layer films were cut using a cutting plotter (CE3000-60, Graphtec). The individual layers are shown in Supplementary Fig. 1. For filtering bacterial cells, a nitrocellulose membrane with a porosity of 0.45 µm (Bio-Rad) was cut using a biopsy punch (14 mm) and assembled in the device as described previously[42]. The chamber underneath the filter was closed using a plastic cover with an injection hole sealed with multiple layers of Parafilm (Bemis Company, Inc.; Supplementary Fig. 7). Before using the device, buffer solution was injected through the hole using a syringe. As the injection hole self-sealed after removing the syringe needle, there was no leakage during operation. Although we used Parafilm in the current prototype device, this can be easily replaced with a custom-designed rubber seal.

Spin characterization. The spin-speed profile of the Dx-FS was quantified using the homemade setup shown in Supplementary Fig. 2. In brief, a 532 nm laser (CPS532-C2; Thorlabs) illuminated a light sensor (LX1972; DFROBOT) configured with an Arduino controller (DFRduino UNO R3; DFROBOT). A Dx-FS was installed in the light path and blocked the light during every spin. The light intensity was acquired at a rate of 6 kHz. The laser-intensity measurements were analysed (Supplementary Fig. 2). We also captured the detailed spinning motion of the Dx-FS using a high-speed camera (Phantom Miro 310; Vision Research). Videos were recorded at 500 frames s^{-1}; still frames are shown in Fig. 1e.

Characterization of the filtration rate of a Dx-FS. To characterize the flow rate in Dx-FS-based filtration, we measured the liquid-decanting time through the membrane at different angular velocities using our home-built spinning platform, as described previously[43]. Briefly, a servo motor (EDB2000-56V24/48-S;

ERAETECH) spun the Dx-FS at the given rotational frequency. Images of the device were captured using a charge-coupled device camera at 5 frames s^{-1}. The motor and camera were synchronized; therefore, photographs were acquired at the same position of the device. The flow volume at a given angular rotational frequency can be estimated by integrating the flow rate over time. The angular rotational frequency reached its maximum at the initial spin of the Dx-FS and decreased over time (Fig. 1f). To understand these conditions, spinning was simulated with a given initial angular rotational frequency with a specific angular acceleration. The flow volume was estimated by integrating the flow rate at the simulated angular rotational frequency (Supplementary Fig. 4). Similarly, the total flow volume from a single spin was estimated from the measured angular rotational frequency of the Dx-FS (Fig. 2c).

Bacterial culture. The *E. coli* strain MG1655, a gift from S.-K. Lee (UNIST), was cultured as described previously[44]. Briefly, the *E. coli* strain was transformed with pGREEN, which encodes the constitutive expression of a green fluorescent protein[45]. Cells were streaked from their stocks on Luria–Bertani agar plates. The plates were incubated at 30 °C for 24 h. Positive clones were selected using ampicillin. The bacterial cells were cultured overnight and then centrifuged for 15 min at 4,000 r.p.m. The culturing medium was discarded and the remaining bacterial pellet was resuspended in 1×PBS. The cells were counted using a haemocytometer. Water, synthetic urine (Biozoa Biological Supply) or urine from a healthy individual were spiked with the desired number of cells for further experiments.

Bacterial cell detection from fluorescence microscopy images. Fluorescently labelled bacterial cells were isolated using a Dx-FS and then imaged using fluorescence microscopy (Figs. 2b and 3b). A sample containing bacteria was processed using a Dx-FS as described earlier. The nitrocellulose membrane from the Dx-FS was transferred to a glass slide. The membrane was embedded in 50% glycerol in water and sealed using a glass coverslip. The membranes were imaged using a standard inverted fluorescence microscope (Eclipse Ti-E; Nikon or IX 71; Olympus) equipped with a motorized stage (for large-area scanning; MS-2000, ASI). Imaging was performed using a ×10 dry objective lens. The bacterial cells in the microscopy images were counted using a wavelet-transform-based spot-detection algorithm[46]. The fluorescence microscopy images were pre-processed by median filtering to remove the salt-and-pepper noise, followed by wavelet-transform-based spot detection with a scale factor of two. All computations were performed using MATLAB (MathWorks).

Colorimetric assay for the detection of bacterial cells. Bacterial counting via the colorimetric assay in the Dx-FS was carried out using a commercial kit (Microbial Viability Assay Kit-WST; Dojindo Molecular Technologies, Inc.) according to the manufacturer's recommended protocols. Briefly, 100 µl of the detection solution (20 µl WST-8 diluted in 80 µl distilled water) was added to the Dx-FS and incubated. Through gentle spinning, the liquid was transported to the top of the membrane and incubated for 45 min at 37 °C. The solution turned a different shade of orange according to the bacterial cell count. To retain the same volume of detection solution on top of the membrane, we removed the liquid from the back chamber before loading the detection solution.

Quantitative analysis of Dx-FS images. In addition to detection of the colorimetric assay in a Dx-FS with the naked eye, images were acquired using photographic devices (a cell phone camera, Apple and a digital single-lens reflex camera, Canon) for more quantitative analyses. Automatic photograph analysis was carried out as follows (Supplementary Fig. 13): we first performed colour calibration of the acquired images using an Imatest eSFR chart, which is the ISO 12233:2014 standard for photograph quality[47]. To measure the colour intensity from the membrane area in a Dx-FS, the regions of interest were found using a template-based cross-correlation analysis from the image. From each region of interest, a circular membrane area was located using a circular Hough transform and the inner-circle pixels were taken (circular region of interest). Colour measurements were carried out by converting the image into the profile connection space L*a*b* (L*, lightness; a*, green-red; and b*, blue-yellow) format[48]. All computations were performed using MATLAB (MathWorks).

Field trials at Kauvery Hospitals in India. For testing our device with patient samples in India, the devices were first fabricated under sterile conditions. Every device was individually inspected for damage and irregularities to avoid failure during the experiment. The devices were then treated with an oxygen plasma and vacuum-sealed to prevent any contamination during transfer. A new device was opened for each sample test, the bottom liquid was injected (Supplementary Fig. 7) and the device was then used. The study was performed under the approval of the Kauvery Hospital Institutional Ethics Committee (IEC; ref. no. KHEC/018/August/Meeting No-002/Proposal no. 002). The samples from the patients were obtained according to the IEC protocol of Kauvery Hospitals India, Pvt., Ltd. (no. ECR/966/Inst/TN/2017). The samples were obtained from Kauvery Hospital, Trichy, and tests were performed at a microbiology laboratory in the hospital. The entire study was registered in the Clinical Trial Registry–India (CTRI/2018/09/015678). The samples were obtained from the patients after obtaining consent for the study. Urine samples were obtained from patients suspected to have a UTI (based on symptoms). The presence of bacteria and their counts were confirmed in the microbiology laboratory at Kauvery Hospital.

Urine culture test. The urine samples obtained from patients were de-identified and a routine culture was performed at the hospital laboratory. Briefly, 1–10 µl urine from a patient was spread onto a BBL trypticase soy agar plate with 5% blood (Kauvery Hospital, India) and, in parallel, a MacConkey plate. The plates were incubated at 37 °C overnight in ambient air and checked for growth on consecutive days; the colony count was confirmed depending on the growth levels. The microorganisms were transferred to glass slides, stained using an acid-fast stain and visualized under a microscope.

Clinical bacterial isolates for AST. All clinical strains used for validating the performance of the AST were isolated from 30 patients at Seoul National University Hospital (SNUH). Clinical samples were obtained and analysed according to the approved institutional review board (IRB) protocol at SNUH (1710-007-889). None of the clinical strains originated from the same patient. Pure cultures of the clinical strains were inoculated on Mueller–Hinton agar plates and incubated for 20–24 h before performing the AST following standard bacterial preparation protocols. After incubation, several colonies were used to prepare bacterial solutions at a concentration of 1.5×10^8 c.f.u. ml^{-1} using DensiChek plus (Biomerieux). Bacterial identification was performed according to the protocols of the hospital where the strain originated, as clinical strains were all identified to be gram-negative by a VITEK 2 system (Biomerieux) at SNUH.

Antimicrobial preparations. The antimicrobial agents were purchased from Sigma Aldrich. The antimicrobial solutions were prepared directly following the manufacturer's instructions with dilution in cation-adjusted Mueller–Hinton broth (BD Biosciences).

Reference AST: broth microdilution test. For the reference AST, we performed a broth microdilution test using antimicrobial solutions in 96-well microtitre plates (BD Biosciences). We inoculated 10 µl bacterial stock solution into the well at a final concentration of 5×10^5 c.f.u. ml^{-1}. Cation-adjusted Mueller–Hinton broth (100 µl) with antimicrobial solutions at the appropriate concentration, recommended by the CLSI, was then introduced. The broth microdilution tests were performed in triplicate. After 16–20 h of incubation at 37 °C, the MIC value of each microdilution well was determined by comparing the amount of growth in the wells containing the antimicrobial agent with the amount of growth in the growth-control wells by unaided visual inspection. A total reduction of growth was considered as non-growth. If the results from the triplicate tests were not identical, the majority result was selected as the MIC.

Fidget-AST. The clinical isolates from 30 UTI patients were de-identified before performing the tests at the Department of Transdisciplinary Studies, Seoul National University, in a blinded manner. *E. coli* samples with predetermined MIC values were selected for the AST using a Dx-FS. For every sample, the bacteria were isolated from the agar plate and diluted to obtain a stock concentration of 1.5×10^8 c.f.u. ml^{-1} as shown in Fig. 5. A final working concentration of 10×10^5 c.f.u. ml^{-1} was transferred to Eppendorf tubes containing antibiotics (CIP, 1 and 4 µg ml^{-1}; and CZ, 16 and 32 µg ml^{-1}) and incubated for 20 min. After the incubation, 1 ml sample was transferred to the Dx-FS sample chamber and enriched on the membrane by spinning. The detection solution was added, incubated for 45 min and the colour intensities were compared. The samples were classified as CIP/CZ-susceptible or -resistant depending on the final colour intensities in comparison to the control sample, which was not treated with antimicrobials. The estimated material cost for a Fidget-AST kit is provided in Supplementary Table 5.

Reporting Summary. Further information on research design is available in the Nature Research Reporting Summary linked to this article.

Data availability

The main data supporting the findings in this study are available within the paper and its Supplementary information. The raw and analysed datasets are too numerous to be readily shared publicly but are available for research purposes from the corresponding author on reasonable request.

Code availability

The custom Matlab code for data analysis is provided at https://github.com/yoonkyoungcho/Fidget.

Received: 15 March 2019; Accepted: 14 April 2020;
Published online: 18 May 2020

References

1. Vashist, S. K., Luppa, P. B., Yeo, L. Y., Ozcan, A. & Luong, J. H. T. Emerging technologies for next-generation point-of-care testing. *Trends Biotechnol.* **33**, 692–705 (2015).

2. Pollock, N. R. et al. A paper-based multiplexed transaminase test for low-cost, point-of-care liver function testing. *Sci. Transl. Med.* **4**, 152ra129 (2012).
3. Ng, A. H. C. et al. A digital microfluidic system for serological immunoassays in remote settings. *Sci. Transl. Med.* **10**, eaar6076 (2018).
4. Watkins, N. N. et al. Microfluidic CD4+ and CD8+ T lymphocyte counters for point-of-care HIV diagnostics using whole blood. *Sci. Transl. Med.* **5**, 214ra170 (2013).
5. Manz, A., Graber, N. & Widmer, H. M. Miniaturized total chemical analysis systems: a novel concept for chemical sensing. *Sens. Actuators B* **1**, 244–248 (1990).
6. deMello, A. J. Control and detection of chemical reactions in microfluidic systems. *Nature* **442**, 394–402 (2006).
7. Whitesides, G. M. The origins and the future of microfluidics. *Nature* **442**, 368–373 (2006).
8. Mauk, M. G. Calling in the test: smartphone-based urinary sepsis diagnostics. *EBioMedicine* **37**, 11–12 (2018).
9. Barnes, L. et al. Smartphone-based pathogen diagnosis in urinary sepsis patients. *EBioMedicine* **36**, 73–82 (2018).
10. Laksanasopin, T. et al. A smartphone dongle for diagnosis of infectious diseases at the point of care. *Sci. Transl. Med.* **7**, 273re1 (2015).
11. S. T. Thomas, C. Heneghan, C. P. Price, A. V. d. Bruel, A. Plüddemann. *Point-of-Care Testing for Urinary Tract Infections. Horizon Scan Report 0045* (National Institute for Health and Research, 2016).
12. Yager, P., Domingo, G. J. & Gerdes, J. Point-of-care diagnostics for global health. *Annu. Rev. Biomed. Eng.* **10**, 107–144 (2008).
13. Michael, I., Kim, T.-H., Sunkara, V. & Cho, Y.-K. Challenges and opportunities of centrifugal microfluidics for extreme point-of-care testing. *Micromachines* **7**, 32 (2016).
14. Posthuma-Trumpie, G. A., Korf, J. & van Amerongen, A. Lateral flow (immuno)assay: its strengths, weaknesses, opportunities and threats. a literature survey. *Anal. Bioanal. Chem.* **393**, 569–582 (2009).
15. Davenport, M. et al. New and developing diagnostic technologies for urinary tract infections. *Nat. Rev. Urol.* **14**, 298–310 (2017).
16. *Urinary Tract Infections in Infants and Children in Developing Countries in the Context of IMCI*. 1–8 (WHO, 2005).
17. Hooton, T. M. Uncomplicated urinary tract infection. *N. Engl. J. Med.* **366**, 1028–1037 (2012).
18. Wilson, M. L. & Gaido, L. Laboratory diagnosis of urinary tract infections in adult patients. *Clin. Infect. Dis.* **38**, 1150–1158 (2004).
19. Gilbert, N. M. et al. Urinary tract infection as a preventable cause of pregnancy complications: opportunities, challenges, and a global call to action. *Glob. Adv. Health Med.* **2**, 59–69 (2013).
20. Schmiemann, G., Kniehl, E., Gebhardt, K., Matejczyk, M. M. & Hummers-Pradier, E. The diagnosis of urinary tract infection. *Dtsch. Aerztebl. Int.* **107**, 361–367 (2010).
21. Foxman, B. The epidemiology of urinary tract infection. *Nat. Rev. Urol.* **7**, 653–660 (2010).
22. Schecter, R. A., Shah, J., Fruitman, K. & Milanaik, R. L. Fidget spinners: purported benefits, adverse effects and accepted alternatives. *Curr. Opin. Pediatr.* **29**, 616–618 (2017).
23. Bhamla, M. S. et al. Hand-powered ultralow-cost paper centrifuge. *Nat. Biomed. Eng.* **1**, 0009 (2017).
24. Zhang, L. et al. Hand-powered centrifugal microfluidic platforms inspired by a spinning top for sample-to-answer diagnostics of nucleic acids. *Lab Chip* **18**, 610–619 (2018).
25. Liu, C. H. et al. Blood plasma separation using a fidget-spinner. *Anal. Chem.* **91**, 1247–1253 (2019).
26. Sackmann, E. K., Fulton, A. L. & Beebe, D. J. The present and future role of microfluidics in biomedical research. *Nature* **507**, 181–189 (2014).
27. Gorkin, R. et al. Centrifugal microfluidics for biomedical applications. *Lab Chip* **10**, 1758–1773 (2010).
28. Kim, T.-H. et al. FAST: size-selective, clog-free isolation of rare cancer cells from whole blood at a liquid-liquid interface. *Anal. Chem.* **89**, 1155–1162 (2017).
29. Tsukatani, T. et al. Comparison of the WST-8 colorimetric method and the CLSI broth microdilution method for susceptibility testing against drug-resistant bacteria. *J. Microbiol. Methods* **90**, 160–166 (2012).
30. Aguiar, J. P. Evaluation of empirical antibiotic therapy for the treatment of community-acquired urinary tract infections (CA-UTI). *Int. Arch. Clin. Pharmacol.* **1**, 002 (2017).
31. *National Treatment Guidelines for Antimicrobial Use in Infectious Diseases, India* 1–64 (National Centre For Disease Control, 2008).
32. Mishra, B., Srivastava, S., Singh, K., Pandey, A. & Agarwal, J. Symptom-based diagnosis of urinary tract infection in women: are we over-prescribing antibiotics? *Int. J. Clin. Pract.* **66**, 493–498 (2012).
33. Hasan, A. S. K., Kumar, N. T., Kishan, R. N. & Neetha, K. Laboratory diagnosis of urinary tract infections using diagnostics tests in adult patients. *Int. J. Res. Med. Sci.* **2**, 415–421 (2014).
34. George, C. E., Norman, G., Ramana, G. V., Mukherjee, D. & Rao, T. Treatment of uncomplicated symptomatic urinary tract infections: resistance patterns and misuse of antibiotics. *J. Fam. Med. Prim. Care* **4**, 416–421 (2015).
35. European Confederation of Laboratory Medicine. European urinalysis guidelines. *Scand. J. Clin. Lab. Invest.* Suppl. **231**, 1–86 (2000)..
36. Chokshi, M. et al. Health systems in India. *J. Perinatol.* **36**, S9–S12 (2016).
37. *Guidelines for Good Clinical Laboratory Practices (GCLP)* (Indian Council of Medical Research, 2008).
38. Kuper, K. M., Boles, D. M., Mohr, J. F. & Wanger, A. Antimicrobial susceptibility testing: a primer for clinicians. *Pharmacotherapy* **29**, 1326–1343 (2009).
39. Avesar, J. et al. Rapid phenotypic antimicrobial susceptibility testing using nanoliter arrays. *Proc. Natl Acad. Sci. USA* **114**, E5787–E5795 (2017).
40. Amábile-Cuevas, C. F. Basis for a cheap method for detecting bacteria and assessing their antibiotic susceptibility in urine samples. *J. Glob. Antimicrob. Resist.* **1**, 17–21 (2013).
41. Kettler, H., White, K. & Hawkes, S. *Mapping the Landscape of Diagnostics for Sexually Transmitted Infections* (UNICEF/UNDP/World Bank/WHO, 2004).
42. Lee, A. et al. All-in-one centrifugal microfluidic device for size-selective circulating tumor cell isolation with high purity. *Anal. Chem.* **86**, 11349–11356 (2014).
43. Lee, B. S. et al. Fully integrated lab-on-a-disc for simultaneous analysis of biochemistry and immunoassay from whole blood. *Lab Chip* **11**, 70–78 (2011).
44. Yaguchi, T. et al. Aqueous two-phase system-derived biofilms for bacterial interaction studies. *Biomacromolecules* **13**, 2655–2661 (2012).
45. Hellens, R. P., Edwards, E. A., Leyland, N. R., Bean, S. & Mullineaux, P. M. pGreen: a versatile and flexible binary Ti vector for *Agrobacterium*-mediated plant transformation. *Plant Mol. Biol.* **42**, 819–832 (2000).
46. Olivo-Marin, J.-C. Extraction of spots in biological images using multiscale products. *Pattern Recognit.* **35**, 1989–1996 (2002).
47. *Photography–Electronic Still Picture Imaging–Resolution and Spatial Frequency Responses* 3rd edn (International Organization for Standardization, 2017).
48. *International Color Consortium Specification ICC.1:2004–10* (ICC, 2006).

Acknowledgements

We thank S. Manivanan for his support in the clinical sample testing. We thank J. Oh for discussions about the modelling. This work is supported by a grant from the Institute for Basic Science of Korea (grant no. IBS-R020-D1) and the Korean Health Technology R&D Project of the Ministry of Health and Welfare (grant no. HI12C1845).

Author contributions

I.M., D.K. and Y.-K.C. conceived and designed the research. I.M., D.K., O.G., Sumit K., J.C., Saravana K., D.Y.K., J.P., H.Y.J. and T.S.K. performed the research. I.M., D.K., O.G., H.Y.J., S.Kwon and Y.-K.C. wrote the manuscript.

Competing interests

I.M., D.K., D.Y.K. and Y.-K.C. are inventors of a patent (10-2103784, Korea). Y.-K.C. is an inventor of a filed patent (14/780,002, USA). All other authors declare no competing interests.

Additional information

Supplementary information is available for this paper at https://doi.org/10.1038/s41551-020-0557-2.

Correspondence and requests for materials should be addressed to Y.-K.C.

Reprints and permissions information is available at www.nature.com/reprints.

Publisher's note Springer Nature remains neutral with regard to jurisdictional claims in published maps and institutional affiliations.

nature research

Corresponding author(s): Yoon-Kyoung Cho

Last updated by author(s): Apr 9, 2020

Reporting Summary

Nature Research wishes to improve the reproducibility of the work that we publish. This form provides structure for consistency and transparency in reporting. For further information on Nature Research policies, see Authors & Referees and the Editorial Policy Checklist.

Statistics

For all statistical analyses, confirm that the following items are present in the figure legend, table legend, main text, or Methods section.

n/a	Confirmed
☐	☒ The exact sample size (*n*) for each experimental group/condition, given as a discrete number and unit of measurement
☐	☒ A statement on whether measurements were taken from distinct samples or whether the same sample was measured repeatedly
☐	☒ The statistical test(s) used AND whether they are one- or two-sided *Only common tests should be described solely by name; describe more complex techniques in the Methods section.*
☐	☒ A description of all covariates tested
☐	☒ A description of any assumptions or corrections, such as tests of normality and adjustment for multiple comparisons
☐	☒ A full description of the statistical parameters including central tendency (e.g. means) or other basic estimates (e.g. regression coefficient) AND variation (e.g. standard deviation) or associated estimates of uncertainty (e.g. confidence intervals)
☐	☒ For null hypothesis testing, the test statistic (e.g. *F*, *t*, *r*) with confidence intervals, effect sizes, degrees of freedom and *P* value noted *Give P values as exact values whenever suitable.*
☒	☐ For Bayesian analysis, information on the choice of priors and Markov chain Monte Carlo settings
☒	☐ For hierarchical and complex designs, identification of the appropriate level for tests and full reporting of outcomes
☒	☐ Estimates of effect sizes (e.g. Cohen's *d*, Pearson's *r*), indicating how they were calculated

Our web collection on statistics for biologists contains articles on many of the points above.

Software and code

Policy information about availability of computer code

Data collection	Fluorescence microscopy images were acquired through a Nikon microscope and the Nikon acquisition software NIS-Elements AR v.5.02.
Data analysis	Custom code in MATLAB 2018b (MathWorks, MA, USA), available at https://github.com/yoonkyoungcho/Fidget.

For manuscripts utilizing custom algorithms or software that are central to the research but not yet described in published literature, software must be made available to editors/reviewers. We strongly encourage code deposition in a community repository (e.g. GitHub). See the Nature Research guidelines for submitting code & software for further information.

Data

Policy information about availability of data

All manuscripts must include a data availability statement. This statement should provide the following information, where applicable:

- Accession codes, unique identifiers, or web links for publicly available datasets
- A list of figures that have associated raw data
- A description of any restrictions on data availability

The main data supporting the findings in this study are available within the paper and its Supplementary Information. The raw and analysed datasets are too numerous to be readily shared publicly, yet they are available for research purposes from the corresponding author on reasonable request.

Field-specific reporting

Please select the one below that is the best fit for your research. If you are not sure, read the appropriate sections before making your selection.

☒ Life sciences ☐ Behavioural & social sciences ☐ Ecological, evolutionary & environmental sciences

Life sciences study design

All studies must disclose on these points even when the disclosure is negative.

Sample size	All experiments were carried out with three independent biological replicates per experiment (details provided in Methods and in the figure legends). On the basis of published work (in particular, Schoepp et al., Sci. Transl. Med. 9, eaal3693, 2017; Banoo et al., Nat. Rev. Microbiol. 4, S21–S31, 2006), we calculated the minimum sample size of the test shown in Figure 4. Assuming that the sensitivity and specificity of Dx-FS are 95%, at least 18.2 (or 19) samples that are positive by the gold-standard test are required to measure the sensitivity within ±10%. In this study, we tested 18 UTI-positive samples and 21 UTI-negative samples.
Data exclusions	No data were excluded from the analyses.
Replication	The Dx-FS assays, including Dx-FS, Fidget-ID and Fidget-AST, were validated with n = 3 and reproduced three times, with similar results.
Randomization	Dx-FS devices were randomly allocated to the samples.
Blinding	All the patient-sample testing using Dx-FS was carried out blindly. The results from Dx-FS were obtained first (within an hour), and the urine culture/urinalysis results were provided by the hospital after two weeks.

Reporting for specific materials, systems and methods

We require information from authors about some types of materials, experimental systems and methods used in many studies. Here, indicate whether each material, system or method listed is relevant to your study. If you are not sure if a list item applies to your research, read the appropriate section before selecting a response.

Materials & experimental systems

n/a	Involved in the study
☐	☒ Antibodies
☒	☐ Eukaryotic cell lines
☒	☐ Palaeontology
☒	☐ Animals and other organisms
☐	☒ Human research participants
☒	☐ Clinical data

Methods

n/a	Involved in the study
☒	☐ ChIP-seq
☒	☐ Flow cytometry
☒	☐ MRI-based neuroimaging

Antibodies

Antibodies used	Biotin-conjugated Rabbit anti-E. coli antibody (Cat#1007, Lot#FF258; ViroStat, USA).
Validation	The anti-E.coli antibody was validated by displaying it to E. coli (positive control) or S. aureus (negative control) with streptavidin labels.

Human research participants

Policy information about studies involving human research participants

Population characteristics	For Dx-FS, urine samples were collected from patients suspected with UTI (on the basis of symptoms). The summary of patient characteristics is given in Supplementary Table 3. Among 39 patients, the characteristics of the participants are as follows: Age (years): age <16 (2, 5%); 16 ≤ age < 25 (4, 10%); 25 ≤ age < 50 (10, 26%); 50 ≤ age < 80 (23, 59%). Gender: male (21, 54%); female (18, 46%). Inpatient/outpatient: inpatient (25, 64%); outpatient (14, 36%). For Fidget-AST, all clinical strains used for validating the AST performance were isolated from 30 patients at Seoul National University Hospital (SNUH). The antibiotic susceptibility profile of the participants are as follows; CIP resistant / CZ resistant (5), CIP resistant / CZ susceptible (5), CIP susceptible / CZ resistant (5), CIP susceptible / CZ susceptible (15). According to the IRB of this study, the tests were done in a blind manner, and other characteristics such as gender or sex were not disclosed.
Recruitment	The urine samples were selected on the basis of two criteria: (1) The patient was symptomatically diagnosed as UTI positive by the doctor, and (2) The sample had to be less than 2 hours old. We believe that this random selection neutralized any bias that may have impacted the sample-selection process. However, since the sample was obtained from 2 branches of the same hospital (within a specific geographic area), there could be a potential bias pertaining to an uneven representation of certain populations. Bacterial identification was performed according to the protocols of the hospital where the strain originated. The samples were

used for the further AST study.

Ethics oversight

The samples from the patients were obtained according to the IEC protocol of Kauvery Hospitals India, Pvt., Ltd. (# ECR/966/Inst/TN/2017). The samples were obtained from Kauvery Hospital, Trichy, and tests were performed at a microbiology lab within the hospital. The entire study was registered in the Clinical Trial Registry India (CTRI/2018/09/015678).

Clinical samples were obtained and analysed according to the approved institutional review board (IRB) protocol at SNUH (1710-007-889).

Note that full information on the approval of the study protocol must also be provided in the manuscript.